Chin. J. Geochem. (2015) 34(1):55–61
DOI 10.1007/s11631-014-0020-8

ORIGINAL ARTICLE

Preparation of Mn_3O_4 from low-grade rhodochrosite ore by chemical bath deposition method

Jing Zhao · Longjun Xu · Taiping Xie · Chao Xie

Received: 23 December 2013 / Revised: 2 March 2014 / Accepted: 5 March 2014 / Published online: 4 February 2015

Abstract Mn_3O_4 was prepared with the chemical bath deposition (CBD) method. A $MnSO_4$ solution was obtained by the leaching and purifying of low-grade rhodochrosite ore (LGRO), which was used as raw material. The preparation procedures were studied and promoted. The results showed that the Mn_3O_4 with the highest purity and highest specific surface area could be obtained under the following processes. An $MnSO_4$ solution of 1.0 mol/L was added into a beaker under a flow rate of 30 mL/h. The pH of the reaction solution was adjusted to 10 using $NH_3{\cdot}H_2O$ at 80 °C. Then the solids were washed and dried at 200 °C for 2.5 h. The total Mn content (TMC) of Mn_3O_4 was 72.0 %. The ionic distributions was formulated as $[Mn^{2+}][Mn^{2+}_{0.3024}Mn^{3+}_{0.2937}\ Mn^{4+}_{0.3786}\square_{0.0254}]_2O_4$. The average crystallite size of Mn_3O_4 with a tetragonal hausmannite structure was found to be about 35 nm by X-ray diffraction (XRD) analysis. The BET specific surface area of the Mn_3O_4 measured was 32 m^2/g.

Keywords Mn_3O_4 · Low-grade rhodochrosite ore · Chemical bath deposition method

J. Zhao (✉) · L. Xu · T. Xie
State Key Laboratory of Coal Mine Disaster Dynamics and Control, Chongqing University, Chongqing 400044, China
e-mail: 20077313@cqu.edu.cn

L. Xu
e-mail: xulj@cqu.edu.cn

C. Xie
School of Environmental Protection and Safety Engineering, University of South China, Hengyang 421001, China

1 Introduction

Mn_3O_4 is widely used as electrode materials (Zhao et al. 2012; Yang et al. 2012; Dubal et al. 2010), soft magnetic materials (Gabriela et al. 2012), catalysts (Li et al. 2009), corrosion-inhibiting pigments, etc. There are many methods for preparation of Mn_3O_4 powders, such as thermal decomposition (Chang et al. 2005), hydrothermal (Zhang et al. 2004a; Ahmed et al. 2011; Yang et al. 2006), solvothermal (Li et al. 2009; Zhang et al. 2004b), microwave assisted (Apte et al. 2006), and ultrasonic irradiation (Gopalakrishnan et al. 2005; Bastami et al. 2012). However, most of these methods were time consuming and uneconomical, in addition to requiring high cost equipment. As compared to these methods, the CBD method was attractive because it was relatively simple and inexpensive.

Past research on the synthesis of Mn_3O_4 by CBD method had been reported. Peng et al. (2010) produced Mn_3O_4 by the aqueous solution oxidation method. Mn_3O_4 nanoparticles were prepared by a simple chemical route, using cetyltetramethyl ammonium bromide (CTAB) as a template agent (Hassouna et al. 2012). Nevertheless, the reaction system in the chemical bath was quite complex and many conditions had a great influence on the characteristics of the products, such as the concentration, pH and temperature of the reaction solution. Chen et al. (2006) reported that the difference in the dripping speed of the NaOH solution leads to a large difference in the Mn_3O_4 morphologies produced. Therefore, the preparation procedures of Mn_3O_4 by CBD method were worth further studying and promoting.

In recent years, more attention has been paid to developing processes for the economical recovery of manganese from low grade manganese ores and other secondary resources (Mehdilo et al. 2013; Zhang and Cheng 2007). In

this paper, LGRO was used as the raw material to produce Mn_3O_4. Firstly, the LGRO was leached with sulfuric acid and purified to obtain the pure $MnSO_4$ solution. Then, the Mn_3O_4 was prepared by the CBD method in two stages. During the first hydrolysis-oxidation stage, the $MnSO_4$ solution was hydrolyzed with NH_3 solution and oxidized by the air to gain the precursor. During the second heating-oxidation stage, the precursor was dried and simultaneously further oxidized by the air. So, the synthetic route of Mn_3O_4 was simplified effectively as compared to the traditional process. In conclusion, this method was simple and inexpensive. Neither complex apparatuses nor sophisticated techniques were required. This study was of great significance to provide a possible high efficiency way for the utilization of LGRO.

2 Experimental

2.1 Materials and apparatus

The LGRO samples weres from Xiushan, Chongqing, and the average composition was described in Table 1.

Chemical reagents mainly included H_2SO_4, NaOH, NH_4Cl, NH_3 solution, $Na_2C_2O_4$, and EDTA, which were of analytical grade. $KMnO_4$ used in this experiment was a guaranteed reagent.

Apparatus included constant temperature bath with mixer (DF-101S), pH meter (pHS-3C), electrothermal blowing dry box(101-1), analysis instrument of specific surface area and pore diameter (ASAP2010, USA) and X-ray diffractometer (Bruker Advance D8).

2.2 Methods

The LGRO was leached with sulfuric acid and filtered (Zhao et al. 2013). After oxidizing Fe^{2+} ions to Fe^{3+} ions with MnO_2 powders, aluminum and iron were removed successively from the filtrate in the form of insoluble salts by adding NaOH solution. Then calcium ions (Ca^{2+}), magnesium ions (Mg^{2+}) and heavy metals were eliminated by the introduction of sulfide and fluoride. The pure $MnSO_4$ solution with 191.16 g/L was obtained. The leaching efficiency of Mn was 96.8 %. The removal rates of iron, calcium, and magnesium were 99.8 %, 99.1 %, and 96.8 %, respectively.

The fresh aqueous solution of 1.5 mol/L NH_3 solution, buffer solution at pH = 10 and $MnSO_4$ solutions at various concentrations were prepared in advance. First, 20 mL of the buffer solution was transferred into a beaker immersed in a constant temperature bath. Then the prepared Mn^{2+} solution was added at different flow rates into the beaker under vigorous stirring and at various temperatures with an aging time of 2 h. Meanwhile, the NH_3 solution was dropwise added to make the Mn^{2+} ions precipitate and to control the pH of the solution. The solid was filtered and carefully washed with distilled water several times to obtain the precursor. This stage was called hydrolysis-oxidation. During this stage, influences of several reaction variables such as concentration and flow rate of the $MnSO_4$ solution, temperature and pH were investigated. Finally, the precursor was dried in an electrothermal blowing dry box at various temperatures for different times, and the product was obtained. This stage was called heating-oxidation, and the precursor was dried and further oxidized by the air simultaneously. During this stage, the effects of the heating temperature and time on the total Mn content (TMC) of the product were studied. All experiments were carried out in ambient conditions under atmosphere with air as an oxidizing agent.

The mole ratio of $MnSO_4$ to NH_3 solution was 5:1 in all experiments. After the quantitative NH_3 solution was used up, a small amount of NaOH solution was introduced to adjust the pH of the reaction solution. This way, the Mn recovery percentage could remain at a high level and the influence of the Na^+ could be controlled effectively.

2.3 Product characterization

With the selective dissolution, potassium permanganate titration and EDTA titration method combined (Yu and Huang 2004), the contents of Mn^{2+}, Mn^{3+}, Mn^{4+} and TMC in the product were determined. Next, cation distributions and lattice constants of the Mn_3O_4 were calculated respectively. The X-ray diffraction (XRD) determination of the structures present in the as-prepared samples was carried out on a Bruker Advance D8 X-ray diffractometer with CuKα radiation ($\lambda = 0.154$ nm) at 40 kV and 30 mA. The scan rate was 4°/min for values of 10°–85°. Brunauer-Emmett-Teller (BET) surface area measurement was performed on Micromeritics ASAP 2010 at 77 K.

Table 1 Chemical composition of LGRO/wt%

Component	Mn	SiO_2	Fe_2O_3	CaO	MgO	Al_2O_3	K_2O	P	S	Other
Content %	12.31	37.94	3.08	7.88	3.99	2.21	2.14	0.25	3.13	27.07

3 Results and discussions

When the pure $MnSO_4$ and NH_3 solution were mixed, the solution became yellow to yellow–brown and precipitation occurred. The reaction scheme was described as following,

$$MnSO_4 + 2NH_3 - H_2O = Mn(OH)_2 + (NH_4)_2SO_4 \quad (1)$$

and the $Mn(OH)_2$ was instable and could transform to Mn_3O_4 by the air.

$$6Mn(OH)_2 + O_2 = 2Mn_3O_4 + 6H_2O \quad (2)$$

During the hydrolysis-oxidation stage, both reactions existed. $MnSO_4$ was hydrolyzed and precipitated as $Mn(OH)_2$. Then most of the $Mn(OH)_2$ produced was oxidized. The residuary one could be further oxidized in heating-oxidation stage.

3.1 Effect of the concentration of MnSO4 solution on the TMC

Five 100 mL $MnSO_4$ solutions of different concentrations were added to the beaker containing the buffer solution under vigorous stirring at a flow rate of roughly 30 mL/h. The precursor was obtained at 60 °C and pH = 10 with an aging time of 2 h, and then dried at 150 °C for 3 h. The TMC in products are shown in Fig. 1. It was around 71 %, which had little to do with the concentration of $MnSO_4$ solution. However, Mn recovery percentage revealed a decreasing trend with the increase of Mn^{2+} ion concentration. When the concentration of $MnSO_4$ solution was higher (1.0 and 1.2 mol/L), $Mn_2(OH)_2SO_4$ was formed and the Mn^{2+} ions were not able to precipitate completely as $Mn(OH)_2$. Meanwhile, it was more difficult to oxidize $Mn_2(OH)_2SO_4$ than $Mn(OH)_2$ by air. Thus, TMC in the products was kept low. Consequently, the concentration of the $MnSO_4$ solution should be not too low or too high but appropriate. So, the Mn recovery percentage could reach 97.3 %.

3.2 Effect of the flow rate of MnSO4 solution on the TMC

In order to study the effect of the flow rate, the $MnSO_4$ solutions were added into the beaker at different flow rates (ranging from 20 to 60 mL/h). The hydrolysis-oxidation were generated at 60 °C and pH = 10. As seen from the results in Fig. 2, the TMC fell considerably with the increase of flow rates. When the $MnSO_4$ solution was quickly dripped into the reaction system (about 50 mL/h), the excessive Mn^{2+} in reaction solution not only lead to an incomplete precipitate, but also resulted in the difficult oxidation of the formed $Mn(OH)_2$. In consequence, high flow rates had adverse effects on both hydrolysis and oxidation. Considering the time factor, the flow rates were chosen to be 40 mL/h. Thus, the TMC was 71.1 %.

3.3 Effect of the temperature on the TMC

To improve the TMC of the product, experiments were carried out at various temperatures. The results in Fig. 3 expose that the TMC rose from 70.2 % at 50 °C to 71.6 % at 90 °C. As the formation and further oxidation of $Mn(OH)_2$ was easier and faster at high temperature, the Mn recovery percentage and TMC of the products were both enhanced. However, the lessening of ammonia due to evaporation at high temperature limited the availability of NH_3 solution. Even worse, the treatment of ammonia vapours was burdensome. Therefore, the optimum temperature was at 80 °C, and with a TMC of 71.6 %.

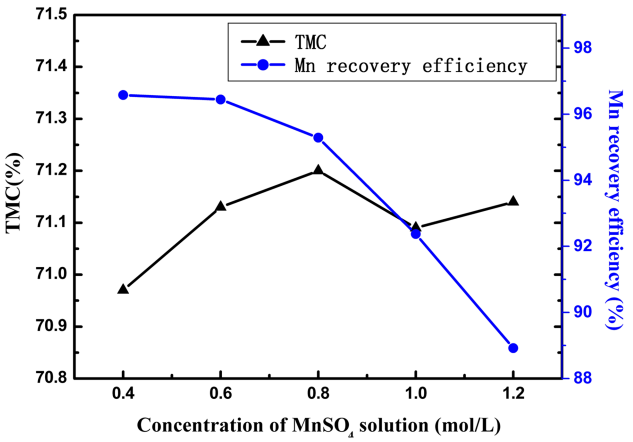

Fig. 1 Effect of concentration of $MnSO_4$ solution on total Mn content

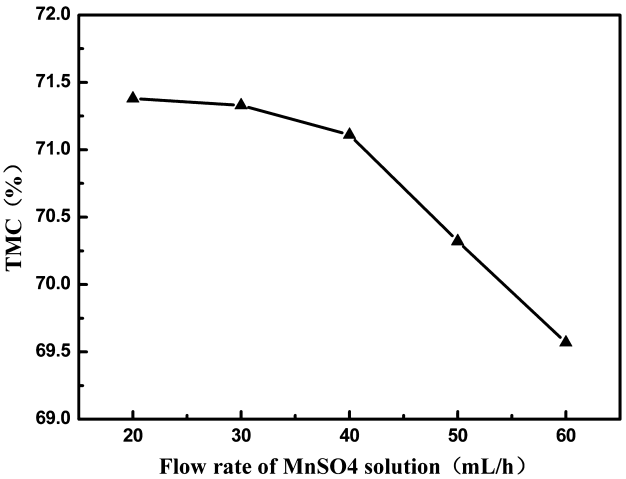

Fig. 2 Effect of flow rate of $MnSO_4$ solution on TMC

3.4 Effect of the pH in reactive system on the TMC

Under the above optimum conditions, various pHs (from 8 to 12) were examined in the hydrolysis-oxidation stage. The results are shown in Fig. 4. It was clear that the curve increased first then decreased, and the highest TMC (71.57 %) was recorded at pH = 10. The TMC was extremely low in the beginning because Mn^{2+} was precipitated and oxidized slowly and difficultly in the weak alkaline reactive system. With the increase of the pH, the rise of TMC was clearly detected. Nevertheless, when the pH was higher than 10 the TMC began to obviously decrease. The reason was that the strong alkaline solution leaded to the over-oxidation of $Mn(OH)_2$. Therefore, the adapted pH of solution was 10.

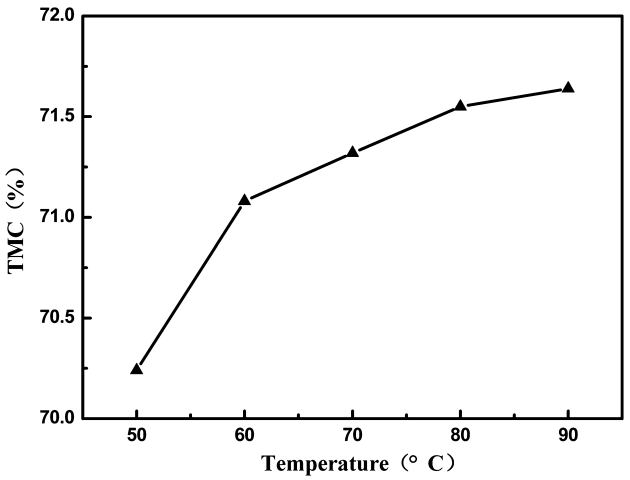

Fig. 3 Effect of temperature on TMC

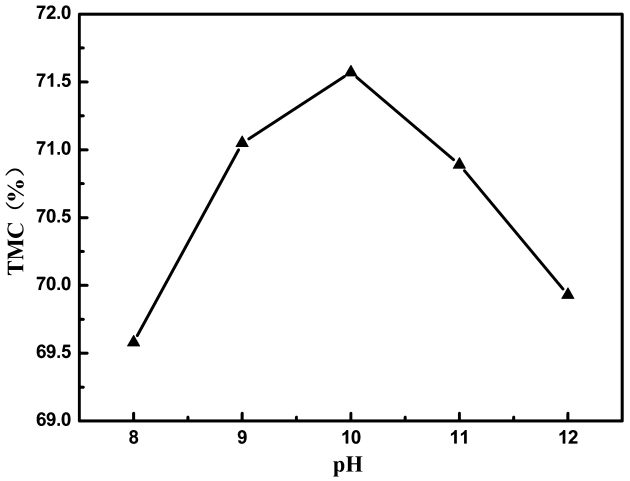

Fig. 4 Effect of pH in reactive system on TMC

3.5 Effects of the heating temperature and time on the TMC

The orthogonal array testing was used to study the influences of concentration and flow rate of the $MnSO_4$ solution, the reaction temperature and the pH on the TMC of the products. The orthogonal array had four factors with three levels. The results indicated that the factor with the biggest effect on the Mn content of the product was temperature, with pH coming in second. The influence of the concentration of $MnSO_4$ solution was minimal. These results were observed from the single-factor testing. The optimum hydrolysis-oxidation parameters of synthesis of Mn_3O_4 were as follows. Concentration of $MnSO_4$ solution was 1.0 mol/L, flow rate of $MnSO_4$ solution was 30 mL/h, reaction temperature was 80 °C, and pH was 10.

According to the single-factor and orthogonal array testing, the TMC could only reach about 71.5 %, even under the optimum hydrolysis-oxidation conditions. Since the theoretical value of TMC of Mn_3O_4 was 72.0 %, the speculation that the residuary $Mn(OH)_2$ was not still oxidized completely was reasonable. Hence, more single-factor experiments were performed to improve the heating-oxidation conditions. The precursors prepared under the optimum hydrolysis-oxidation conditions were dried at 100–200 °C for 3 h. In Fig. 5, the largest TMC was observed when the temperature went up to 200 °C. Then the precursors were dried at 200 °C for a different time, and the results were revealed in Fig. 6. It was found that the TMC increased with the increase of temperature and time. $Mn(OH)_2$ was instable, and could be further oxidized to Mn_3O_4 during the drying process. That was why the curves in Figs. 5 and 6 both increased. The $Mn(OH)_2$ could

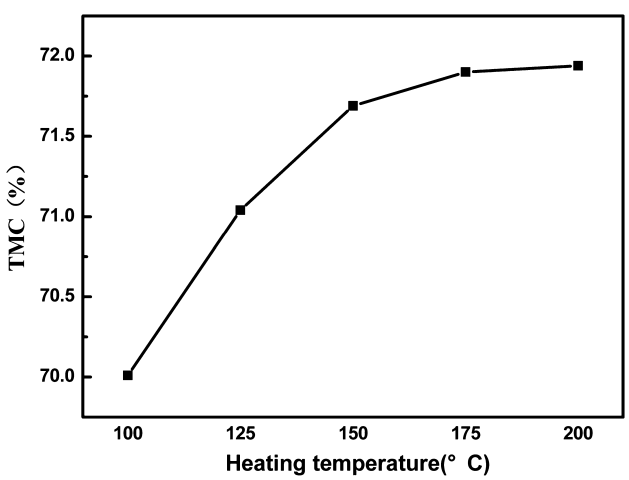

Fig. 5 Effect of heating temperature on TMC

be almost entirely transformed to Mn_3O_4 when it was dried at 200 °C for 2.5 h. The TMC of the product reached 72.0 %.

3.6 Characterization of the product (Mn3O4)

3.6.1 Ionic distribution

The products were prepared under the optimum hydrolysis-oxidation and heating-oxidation conditions. The contents of Mn^{2+}, Mn^{3+}, Mn^{4+} and TMC in the products were determined and listed in Table 2. The highest total content of Mn (exceeding 72.0 %) indicated that the as-prepared samples were in a high purity.

As is well known, Mn_3O_4 was a kind of mixed oxide. But there were three different ways to denote it. One view believed that the form of Mn_3O_4 was $MnO{\cdot}Mn_2O_3$ including both Mn^{2+} ions and Mn^{3+} ions. The second point argued that Mn_3O_4 was $2MnO{\cdot}MnO_2$ containing both Mn^{2+} ions and Mn^{4+} ions. The third stated that Mn_3O_4 was consist of $2MnO{\cdot}MnO_2$ in surface and $MnO{\cdot}Mn_2O_3$ inside, and it included Mn^{2+}, Mn^{3+} and Mn^{4+} ions. Gopalakrishnan et al. (2005) reported the ionic structure of Mn_3O_4 synthesized by ultrasonic irradiation was $[Mn^{2+}][Mn^{3+}]_2O_4$. Yu and Huang (2004) confirmed the structural formula of Mn_3O_4 was $2MnO{\cdot}MnO_2$. Xiong et al. (2000) proposed the possible distribution of various ions in Mn_3O_4 was $[Mn^{2+}][Mn^{2+}_{0.3098}\ Mn^{3+}_{0.2742}Mn^{4+}_{0.3894}\square_{0.0266}]_2O_4$.

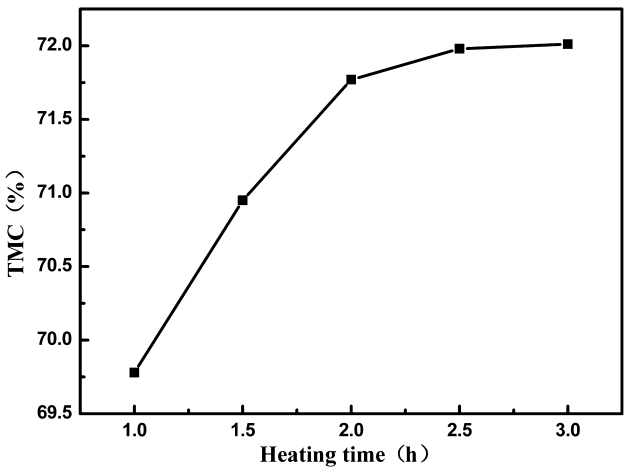

Fig. 6 Effect of heating time on TMC

Table 2 Content of different manganese ions and TMC in the products (%, w/w)

Samples	Mn^{2+} (%)	Mn^{3+} (%)	Mn^{4+} (%)	TMC (%)
1	39.24	14.50	18.26	72.0
2	39.36	14.01	18.65	72.0
3	38.96	13.51	18.56	72.0

The valence state of the manganese in the as-prepared Mn_3O_4 contained Mn^{2+}, Mn^{3+} and Mn^{4+} ions. Based on the spinel structures and the contents of different manganese ions in Mn_3O_4, the ionic distributions were formulated as $[Mn^{2+}][Mn^{2+}_{0.3024}Mn^{3+}_{0.2937}Mn^{4+}_{0.3786}\square_{0.0254}]_2O_4$, which was in good agreement with the previous report (Xiong et al. 2000). According to the ionic distributions and the previous report (Laarj et al. 1996), the lattice constants of the as-prepared product were calculated as $a_T = 0.5741$ nm and $c_T = 0.9375$ nm, which was consistent with the parameters ($a = b = 0.5750$ nm, $c = 0.9420$ nm) in JCPDS card of Mn_3O_4 (JCPDS No.024-0734).

3.6.2 Crystal structure of Mn_3O_4

The X-ray diffraction pattern of the product is presented in Fig. 7. All the diffraction peaks were successfully refined with the tetragonal hausmannite crystal structure model (JCPDS No.024-0734) of Mn_3O_4. No peaks of impurities were detected. Thus, the product obtained by CBD method from LGRO was confirmed pure γ-Mn_3O_4 with tetragonal phase. The lattice constants were determined, i.e. $a = b = 0.5758$, $c = 0.9462$ nm. It was in harmony with the calculated above and the value in JCPDS card. Hassouna et al. (2012) reported the preparation of Mn_3O_4 with a crystallite size between 20 and 80 nm using the precipitation method. Anilkumar and Ravi (2005) prepared the nanocrystalline Mn_3O_4 with the average particle size of $\sim$50 nm by gel to crystalline method. The average grain size of the as-prepared Mn_3O_4 was calculated. The result was about $\sim$35 nm.

3.6.3 Specific surface area of Mn_3O_4

Specific surface area of Mn_3O_4 was determined using the multi-point BET method of adsorption of nitrogen gas

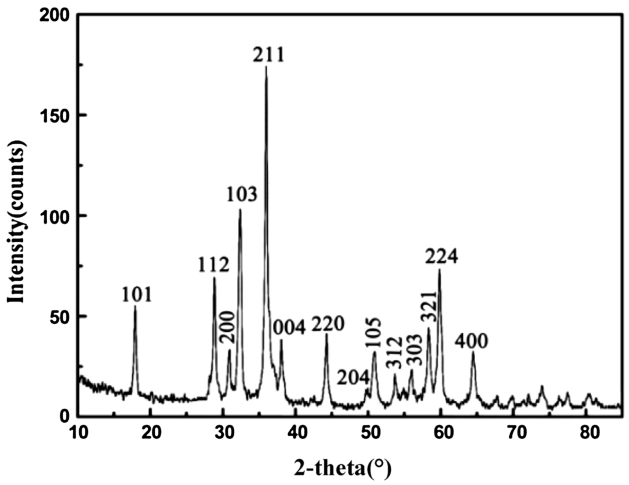

Fig. 7 Diffraction analysis of the Mn_3O_4

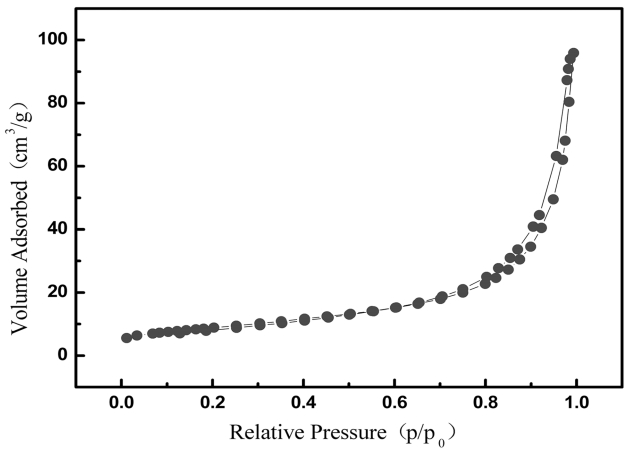

Fig. 8 Physisorption isotherm of the Mn_3O_4

(ASAP 2010). The physisorption isotherm was in Fig. 8. The adsorption and desorption isotherms showed a hysteresis loop in the relative pressure (P/P_0) ranging from 0.70 to 0.98, which was associated with capillary condensation taking place in the mesopores, and the limiting uptake over a range of high P/P_0. Therefore, the Mn_3O_4 exhibited adsorption isotherm of Type *IV* and the product was mesoporous material. The BET surface area and average pore diameter of the as-prepared Mn_3O_4 were 32 m^2/g and 15.8 nm, respectively. The average particle size could been calculated with the formula,

$$Q = 6/(\rho \times S) \quad (3)$$

where ρ is the theoretical density of the Mn_3O_4 materials (4.86 g/cm^3) and S is the specific surface area of the product. The particle size of the product was 38 nm, which was just slightly bigger than that displayed from the XRD.

4 Conclusions

Mn_3O_4 with high specific surface area was successfully synthesized by CBD method. The $MnSO_4$ solution was obtained by leaching and purifying of LGRO. The CBD method was composed of two stages. During the hydrolysis-oxidation stage, the $MnSO_4$ solution was hydrolyzed with NH_3 solution and oxidized by the air to gain the precursor. During the heating-oxidation stage, the precursor was dried and further oxidized by the air simultaneously. The synthetic route of Mn_3O_4 was simplified effectively and inexpensively as compared with the traditional process. Neither complex apparatuses nor sophisticated techniques were required. The preparation process of fine Mn_3O_4 provided a potential use for the LGRO.

Through the single-factor and orthogonal array testing, the optimum conditions for synthesis of Mn_3O_4 were obtained. The $MnSO_4$ solution of 1.0 mol/L was added into beaker under a flow rate of 30 mL/h. The pH of the reactive system was adjusted to 10 using NH_3 solution at 80 °C. Then the solids were washed and dried at 200 °C for 2.5 h. The Mn_3O_4 with high purity and high specific surface area was obtained and the TMC of Mn_3O_4 was 72.0 %. The ionic distribution form was $[Mn^{2+}][Mn^{2+}_{0.3024}Mn^{3+}_{0.2937}Mn^{4+}_{0.3786}\square_{0.0254}]_2O_4$. XRD analysis confirmed the tetragonal hausmannite structure with an average crystallite size of ~35 nm. BET specific surface areas reached to 32 m^2 /g.

Acknowledgments The study is financially supported jointly by the Bureau of Land Resources and Housing Management of Chongqing (Scientific & Technologic Program in 2011).

References

Ahmed KAM, Peng H, Wu K, Huang K (2011) Hydrothermal preparation of nanostructured manganese oxides (MnO_x) and their electrochemical and photocatalytic properties. Chem Eng J 172:531–539

Anilkumar M, Ravi V (2005) Synthesis of nanocrystalline Mn3O4 at 100 °C. Mater Res Bull 40:605–609

Apte SK, Naik SD, Sonawane RS, Kale BB, Pavaskar N, Mandale AB, Das BK (2006) Nanosize Mn_3O_4(Hausmannite) by microwave irradiation method. Mater Res Bull 41:647–654

Chang YQ, Yu DP, Long Y, Xu J, Luo XH, Ye RC (2005) Large-scale fabrication of single-crystalline Mn_3O_4 nanowires via vapor phase growth. J Cryst Growth 279:88–92

Chen ZW, Lai JKL, Shek CH (2006) Shape-controlled synthesis and nanostructure evolution of single-crystal Mn_3O_4 nanocrystals. Scr Mater 55:735–738

Dhaouadi H, Ghodbane O, Hosni F, Touati F (2012) Mn_3O_4 nanoparticles: synthesis, characterization, and dielectric properties. ISRN Spectrosc 10:1–8

Dubal DP, Dhawale DS, Salunkhe RR, Fulari VJ, Lokhande CD (2010) Chemical synthesis and characterization of Mn_3O_4 thin films for supercapacitor application. J Alloy Compd 497:166–170

Gopalakrishnan IK, Bagkar N, Ganguly R, Kulshreshtha SK (2005) Synthesis of super paramagnetic Mn_3O_4 nanocrystallites by ultrasonic irradiation. J Cryst Growth 280:436–441

Laarj M, Kacim S, Gillot B (1996) Cationic distribution and oxidation mechanism of trivalent manganese ions in submicrometer $Mn_xCoFe_{2-x}O_4$ spinel ferrites. J Solid State Chem 125:67–74

Li X, Zhou L, Gao J, Miao H, Zhang H, Xu J (2009) Synthesis of Mn_3O_4 nanoparticles and their catalytic applications in hydrocarbon oxidation. Powder Technol 190:324–326

Mehdilo A, Irannajad M, Hojjati-rad MR (2013) Characterization and beneficiation of Iranian low-grade manganese ore. Physicochem Probl Miner Process 49(2):725–741

Peng T, Xu L, Chen H (2010) Preparation and characterization of high specific surface area Mn_3O_4 from electrolytic manganese residue. Central Eurpean J Chem 8:1059–1068

Rohani Bastami T, Entezari MH (2012) A novel approach for the synthesis of superparamagnetic Mn_3O_4 nanocrystals by ultrasonic bath. Ultrason Sonochem 19:560–569

Silva GC, Almeida FS, Ferreira AM, Ciminelli VST (2012) Preparation and application of a magnetic composite (Mn_3O_4/Fe_3O_4) for removal of As(III) from aqueous Solutions. Mater Res 15(3):403–408

Xiong Q, Huang K, Liu S (2000) Study on determination of Mn^{2+}, Mn^{3+}, Mn^{4+} and their distribution in tetragonal spinel-type Mn_3O_4. Chin J Anal Lab 19(5):68–70 (in Chinese with English abstract)

Yang Z, Zhang Y, Zhang W, Wang X, Qian Y, Wen X, Yang S (2006) Nanorods of manganese oxides: synthesis, characterization and catalytic application. J Solid State Chem 179:679–684

Yang G, Li Y, Ji H, Wang H, Gao P, Wang L, Liu H, Pinto J, Jiang X (2012) Influence of Mn content on the morphology and improved electrochemical properties of Mn_3O_4|MnO@carbonnanofiber as anode material for lithium batteries. J Power Sources 216:353–362

Zhang W, Cheng C (2007) Manganese metallurgy review. Part I: leaching of ores/secondary materials and recovery of electrolytic/chemical manganese dioxide. Hydrometallurgy 89:137–159

Yu KP, Huang BG (2004) Valence state of manganese in manganomanganic oxide and analytical method for its paste sample. Min Metall Eng 24(1):58–60, 63 (in Chinese with English abstract)

Zhang W, Yang Z, Liu Y, Tang S, Han X, Chen M (2004a) Controlled synthesis of Mn_3O_4 nanocrystallites, MnOOH nanorods by a solvothermal method. J Cryst Growth 263:394–399

Zhang YC, Qiao T, Ya Hu X (2004b) Preparation of Mn_3O_4 nanocrystallites by low-temperature solvothermal treatment of γ-MnOOH nanowires. J Solid State Chem 177:4093–4097

Zhao Y, Nie U, Wang H, Tian J, Ning Z, Li X (2012) Direct synthesis of palladium nanoparticle s on Mn_3O_4 modified multi-walled carbon nanotubes: a highly active catalyst for methanol electrooxidation in alkaline media. J Power Sources 218:320–330

Zhao J, Xu L, Xie C (2013) Preparation of chemical manganese dioxide from low-grade rhodochrosite ore. Chin J Geochem 32:380–384